https://doi.org/10.17221/20/2026-PSE

Nitrogen application rates mediate rice cooking quality by interfering with root anatomical and senescence physiological traits

*Li Wang, Jing Cao, Hao Cheng, Qinyao Meng, Haojing Li, Guowei Xu**

College of Agriculture, Henan University of Science and Technology, Luoyang, Henan, P.R. China
Li Wang and Jing Cao contributed equally to this work.
**Corresponding author: gwxu2007@163.com*

Citation: Wang L., Cao J., Cheng H., Meng Q.Y., Li H.J., Xu G.W. (2026): Nitrogen application rates mediate rice cooking quality by interfering with root anatomical and senescence physiological traits. Plant Soil Environ., 72: 172–193.

Abstract: Nitrogen fertiliser is a key determinant of rice yield and grain quality; however, the synergistic mechanisms through which nitrogen regulates root anatomical structure, physiological traits, and cooking quality in rice varieties with different eating properties remain unclear. In this study, a pot experiment was conducted using two moderate-eating-quality cultivars (Xudao 3 and Huageng 9) and two superior-eating-quality cultivars (Zhengdao C42 and Nangeng 9308) under four nitrogen levels (0, 0.59, 1.18, and 1.76 g/pot, designated as N0, N1, N2, and N3, respectively). Cooking quality was assessed by amylose content, gel consistency, and alkali spreading value. The results demonstrated that, with increasing nitrogen application, amylose content, alkali spreading value, malondialdehyde (MDA) content, root aerenchyma area, and aerenchyma proportion decreased initially, then increased, reaching their lowest values at the N2 level. In contrast, gel consistency, root antioxidant enzyme activities (SOD, POD, CAT), photosynthetic rate and cortical living cell proportion increased first and then decreased, peaking at N2 treatment. Compared with moderate-eating-quality varieties, superior-eating-quality varieties exhibited significantly lower amylose content, alkali spreading value, MDA content, and aerenchyma proportion, but higher gel consistency, living cell proportion, stele-to-root diameter ratio, antioxidant enzyme activities, and photosynthetic rate. Correlation analysis revealed that root antioxidant enzyme activities, stele diameter and living cell proportion were negatively correlated with amylose content, but positively correlated with gel consistency. Conversely, MDA content, aerenchyma area and aerenchyma proportion showed opposite correlation patterns. These findings indicate that an appropriate nitrogen application rate (1.18 g/pot) enhances root physiological activity, optimises root anatomical structure, and ensures sufficient source supply to the grain sink, thereby synergistically improving cooking quality – an effect particularly pronounced in high-eating-quality rice varieties.

Keywords: *Oryza sativa* L.; nutrition; root senescence; nitrogen application level; root anatomy; root physiological property

Rice (*Oryza sativa* L.), a staple crop of global importance, serves a dual role in ensuring food security and meeting nutritional needs worldwide (Fukagawa and Ziska 2019, Bin Rahman and Zhang 2023). In recent years, the expanded cultivation of high-quality rice cultivars has shifted the focus of both producers and consumers from yield alone to grain quality. Consequently, scientific nitrogen management has

---

Supported by the grants of the National Natural Science Foundation of China, Project No. U1304316; by the Joint Research Fund for Science and Technology Development of Henan Province, Project No. 242103810031; by the Scientific and Technological Research Projects in Henan Province, Project No. 242102110169; by the Open Foundation for Key Laboratory of Cultivation and Physiology of Jiangsu Province, Project No. 027388003K11009, and by the Doctoral Research Initiation Fund Project of Henan University of Science and Technology, Project No. 13480108.

become a critical agronomic strategy for synergistically enhancing both yield and quality (Huang et al. 2020, Dou et al. 2024). As an essential nutrient for plant growth and development, nitrogen is a key component of numerous enzymes and phytohormones and plays an extensive role in regulating metabolic processes (Firouzi 2015, Koper et al. 2025). Nitrogen supply levels directly influence rice growth dynamics and final grain cooking quality (Liang et al. 2022, Hou et al. 2024). Insufficient nitrogen suppresses root development and photosynthetic efficiency, thereby impairing grain cooking quality. Conversely, excessive nitrogen stimulates vegetative overgrowth, disrupts the grain carbon-nitrogen balance, and reduces both yield and cooking quality due to inefficient utilisation of photosynthetic assimilates (Singh et al. 2011, Song et al. 2024, Owusu et al. 2025). Furthermore, nitrogen loss from agroecosystems intensifies environmental eutrophication (Liu et al. 2024, Bulas et al. 2025). Therefore, improving nitrogen use efficiency is imperative for achieving high-yielding, superior-quality rice production and advancing sustainable agricultural development.

As the central organ for nutrient and water uptake in plants, the root system depends on its anatomical architecture as a fundamental morphological basis that reflects both developmental progress and physiological functionality (Xu et al. 2020, Galindo-Castañeda et al. 2022, Duan et al. 2023, Eweda et al. 2025). During nitrogen acquisition and utilisation in crops, the developmental state of anatomical features such as the root cortex, stele, and aerenchyma directly governs the efficiency of water and nutrient absorption and transport (Zhang et al. 2020, Lynch et al. 2023, Srivastava et al. 2025). Previous research has indicated that optimal nitrogen supply promotes an increase in adventitious root diameter and a greater proportional stele area (Zhang et al. 2020, Li et al. 2022, Liu et al. 2024, Eweda et al. 2025). In contrast, low nitrogen stress induces adaptive anatomical remodeling in roots, initially triggering cortical thickening and an increased number of cell layers to expand the absorptive surface, but ultimately resulting in a reduced cross-sectional area, fewer living cells, and premature aerenchyma development – changes that collectively diminish uptake capacity (De Bauw et al. 2019, Li et al. 2022, Srivastava et al. 2025). Notably, root anatomical traits vary significantly among rice genotypes (Chen et al. 2024, Dai et al. 2024). Salsinha et al. (2023) observed that drought-tolerant varieties typically exhibit smaller root diameter, reduced stele and xylem diameters, narrower cortical radius, and thicker cell walls. However, existing studies have largely focused on the physiological responses of individual varieties under varying nitrogen regimes (Uga et al. 2009, Zhen et al. 2020, Salsinha et al. 2023, Eweda et al. 2025). There remains a systematic knowledge gap regarding how root anatomical structures differ among rice varieties with distinct eating-quality profiles under varying nitrogen supplies, and how these structural adaptations subsequently regulate root senescence and the formation of final grain cooking quality.

Root senescence – an irreversible physiological decline in plants – is fundamentally regulated by genetically programmed processes (Liu et al. 2023, Wang et al. 2023, Averill-Bates 2024). It functions as a resource-optimisation strategy, wherein plants selectively degrade macromolecules in ageing roots and remobilise nutrients to developing grains, thereby enabling efficient nutrient recycling (Xin et al. 2021, Averill-Bates 2024, Meng et al. 2024). Consequently, this process critically determines nutrient-use efficiency and directly influences final crop yield and cooking quality (Wang et al. 2023, Wei et al. 2025). Nitrogen supply serves as a major external modulator of root senescence. Compared to nitrogen-deficient conditions, moderate application enhances antioxidant enzyme activity, improving reactive oxygen species (ROS) scavenging capacity (Zhou and Yang 2023, Tavu and Redillas 2025). Typically, activities of root enzymes such as catalase (CAT) exhibit an initial increase followed by a decline with elevating nitrogen levels, whereas malondialdehyde (MDA) content is suppressed – evidence that optimal nitrogen availability helps delay senescence (Liu et al. 2018, Xu et al. 2021, Zhao et al. 2025). Conversely, excessive nitrogen disrupts oxidative homeostasis, aggravates oxidative damage, and ultimately accelerates senescence, thereby compromising root structure and function (Chu et al. 2022, Wei et al. 2025). Notably, significant variations exist among different cultivars (Subudhi et al. 2020, Khan et al. 2021, Liu et al. 2023). For instance, Liu et al. (2023) reported that a nitrogen-sensitive rice variety exhibited significantly higher root oxidation activity than a nitrogen-insensitive variety, reaching a peak at a nitrogen rate of 180 kg/ha, and that this activity showed a significant positive correlation with yield in their study. This finding, however, may be variety- and environment-specific, and the optimal nitrogen rate for peak root activity can vary across genotypes and growing conditions (Chu et al. 2022). However, research on the physiological divergence in root senescence among rice varieties with distinct eating quality under nitrogen regulation, and its linkage to grain cooking quality, remains scarce. In particular, the relationship between root anatomical traits and the senescence process remains unclear.

This study aimed to test the hypothesis that under optimal nitrogen management, rice plants can enhance cooking quality by modulating root anatomical and senescence-physiological traits, and that this regulatory effect may be more pronounced in superior eating-quality cultivars. We systematically evaluated key root anatomical traits – including the area and proportion of root aerenchyma, the area and proportion of living cells, stele diameter, and the stele-to-root diameter ratio – along with senescence-associated physiological parameters: the activities of superoxide dismutase and catalase, and the content of malondialdehyde. The root traits assessed in this study – governing absorption, transport, and senescence resistance – serve as the functional basis of the "flow" process in the "source-sink-flow" system. Variations in these traits directly influence the physiological conditions that determine rice cooking quality. Leaf photosynthetic rate was determined as an indicator of source strength, which determines the amount of carbohydrates available for grain filling and ultimately affects cooking quality. Cooking quality is characterised by three key parameters: amylose content (AC), which determines texture – lower AC is associated with softer, more palatable rice; gel consistency (GC), where a softer (longer) gel is preferred; and alkali spreading value (ASV), which reflects gelatinisation temperature – intermediate-to-high ASV (indicating low GT) is desirable for energy-efficient cooking and smoother texture. The findings are expected to provide the physiological and anatomical foundations for targeted breeding of high-quality, palatable rice varieties and for the development of efficient nitrogen management strategies.

MATERIAL AND METHODS

Plant materials. The experiment was conducted at the research station of Henan University of Science and Technology in Henan Province, China (34°39'N, 112°26'E). Four rice cultivars commonly grown in the region were selected as test materials based on a pre-experiment. They were divided into two groups according to taste scores measured using a Satake rice taste analyser: Xudao 3 and Huageng 9 (moderate eating quality, 70–75 points) and Zhengdao C42 and Nangeng 9308 (superior eating quality, > 85 points). The experiment was carried out during the rice growing seasons of 2023 and 2024. Seeds were sown in a seedling nursery on May 10, 2023, and May 11, 2024, with young seedlings transplanted into pots on June 10, 2023, and June 11, 2024, respectively. The soil used in the pots was a clay loam [Typic fluvaquents, Entisols (US taxonomy)], which had the following properties: in 2023, alkali-hydrolysable nitrogen was 102.8 mg/kg, available phosphorus 4.9 mg/kg, available potassium 115.3 mg/kg, and organic carbon 11.08 g/kg; in 2024, these values were 105.1 mg/kg, 5.2 mg/kg, 118.6 mg/kg, and 11.19 g/kg, respectively. Each pot (25 cm in diameter × 30 cm height) was filled with 15 kg of soil and planted with three hills, each containing two seedlings. Each treatment was replicated 25 times (25 pots). The main growth stages – mid-tillering, panicle initiation, heading, and maturity – were recorded based on plant morphological development. Panicle initiation was determined by microscopic examination of the growing point, heading was recorded when 50% of panicles had emerged, and maturity was determined when 95% of grains had turned yellow.

Treatments. The experiment was a fully randomised block design. Four nitrogen (N) application rates were set in the experiment based on our previous study: 0, 0.59, 1.18, and 1.76 g of N per pot, designated as N0, N1, N2, and N3, respectively. Total superphosphate (5.89% P) and potassium chloride (43% K) were applied as base fertilisers. Phosphorus and potassium fertiliser application rates were uniform across all treatments at 1.32 g P/pot and 0.83 g K/pot, respectively. Nitrogen fertiliser (urea) was applied in four splits: 30% as basal at pre-transplanting (1 day before transplanting), 30% at the recovering stage (7 days after transplanting, DAT), and 20% at spikelet-promoting (applied at the leaf age of remainder 3.5) and 20% at spikelet-preserving (applied at the leaf age of remainder 1.5). From transplanting to maturity, specific irrigation regimes were maintained. A shallow water layer of 2–3 cm was kept during the plant recovery stage. Thereafter, plants were re-irrigated to a 2–3 cm water depth when the soil water potential at 15 cm depth reached –20 kPa; this was continued until one week before final harvest, except for a drainage period during the late tillering stage (Zhang et al. 2025). Pots were covered with a removable rain shelter during rainfall. Soil water potential in each plot was monitored using soil moisture tension meters (Nanjing Institute of Soil Science, Chinese Academy of Sciences, China). Weeds were manually removed, and pesticides were applied as needed to control diseases and insect pests throughout the growing season in both years.

Sampling and measurements

Sampling. Samples were collected at four key growth stages: the mid-tillering stage, panicle initiation stage, heading stage, and maturity stage. For each stage, three pots of plants were randomly selected from each treatment as biological replicates. Briefly, the soil adhering to the roots was gently rinsed with running water, followed by thorough washing with distilled water to remove residual soil particles. The cleaned roots were blotted dry with filter paper to obtain root samples. The samples were flash-frozen in liquid nitrogen for 30 s and then stored at –80 °C for subsequent analysis of root physiological activity.

Measurements of cooking quality. The mature rice grains were stored for three months after harvest. Subsequently, all samples underwent threshing and winnowing processes. Following the principles of randomisation and representativeness, 100 g of sieved rice was precisely weighed and loaded into the sample tray. The DA-7250 near-infrared spectrometer (Perten Instruments AB, Stockholm, Sweden) used in this study was calibrated with the rice-specific calibration model (Model No. RICE01) provided by the manufacturer, which is optimised for determining rice amylose content, gel consistency, and alkali spreading value, with the correlation coefficient (R^2) of the model all > 0.95 and the root mean square error (RMSE) < 0.5. All analyses for these indicators were carried out according to the method described by Dou et al. (2024).

Measurements of taste score. The rice taste analyser used was Satake STA1B (Satake Co., Ltd., Hiroshima, Japan) with the built-in model version V3.0 (optimised for japonica and mid-indica rice in the Yellow River Huaihe River region of China). The taste score is a comprehensive index based on 8 indicators, including amylose content, protein content, gel consistency, and viscosity, with a full score of 100. Varieties with a score of 70–75 points are defined as moderate-eating-quality rice, and those with a score of > 85 points are superior-eating-quality rice (consistent with the local high-quality rice classification standard of Henan Province, China).

Superoxide dismutase, peroxidase, catalase and malondialdehyde enzyme activity. Rice root samples (0.2 g) were homogenised on ice using a pre-chilled mortar and pestle with 10 mL of 0.05 mol/L phosphate buffer (pH 7.8) containing 1% (*w*/*v*) polyvinylpyrrolidone (PVP). The homogenate was centrifuged at 12 000 rpm for 15 min at 4 °C, and the supernatant was collected as the enzyme extract for subsequent assays of superoxide dismutase, peroxidase, and catalase activities.

The determination method of SOD activity was determined according to Gharsallah et al. (2016) using the nitroblue tetrazolium (NBT) photoreduction method. The 3 mL reaction mixture contained 13 mmol/L methionine, 75 mmol/L nitroblue tetrazolium chloride (NBT), 2 μmol/L riboflavin, 10 μmol/L EDTA, and 0.05 mol/L phosphate buffer (pH = 7.5). One unit of SOD activity was defined as the amount of enzyme required to inhibit the photochemical reduction of NBT by 50%. Activity was expressed as units per gram fresh weight (U/g FW).

Peroxidase activity was assayed following the protocol described by Sachadyn-Król et al. (2016). The reaction mixture (5 mL) contained 0.05 mol/L phosphate buffer (pH 5.5), 0.05 mol/L guaiacol, 2% (*v*/*v*) hydrogen peroxide (H_2O_2), and 20% (*w*/*v*) trichloroacetic acid (TCA). The enzyme solution, boiled for 5 min to inactivate endogenous POD, served as the blank control. Absorbance was measured at 470 nm using a microplate reader, and POD activity was expressed as U/(g·min) on a fresh weight (FW) basis.

CAT activity was determined using the method described by Turk et al. (2014). The 3 mL reaction system consisted of 1 mL 0.3% (*v*/*v*) H_2O_2, 1.35 mL distilled water, and 0.65 mL of enzyme extract. The reaction was initiated by the addition of the enzyme extract, with the enzyme solution boiled for 2 min (to inactivate endogenous CAT) serving as the control. The decrease in absorbance was recorded at 240 nm using a spectrophotometer, and CAT activity was expressed as U/g/min FW.

Root malondialdehyde content was determined using the thiobarbituric acid (TBA) method (Velikova et al. 2000). Briefly, 0.2 g of root tissue was ground in a mortar and homogenised in 5 mL of 5% trichloroacetic acid (TCA). The homogenate was centrifuged at 12 000 rpm for 15 min at 4 °C, and the resulting supernatant was retained for subsequent assays. Root tissue (0.2 g) was homogenised in 5 mL of 5% (*w*/*v*) trichloroacetic acid (TCA) and centrifuged at 12 000 rpm for 15 min at 4 °C. Subsequently, 300 µL of 0.6% (*w*/*v*) TBA was added to the supernatant. The mixture was heated in a boiling water bath for 15 min. After rapid cooling, the solution was centrifuged again. The absorbance of the final supernatant was measured at 532, 600, and 450 nm to calculate the MDA content.

Photosynthesis rate. At the heading and maturity stages, six representative rice plants were selected from each treatment. The net photosynthetic rate of flag leaves was measured between 9:00 and 11:00 on a clear day using a LI-COR 6800 portable photosynthesis system (LI-COR Biosciences, Lincoln, USA).

Root anatomical structure. In accordance with Yang et al. (2012), newly developed adventitious roots (8–10 cm in length) were sampled at panicle initiation, a critical stage when root anatomy is stable and optimally regulates subsequent nutrient uptake and transport. Cross-sections were obtained at a position 2 cm from the root tip and imaged using a JSM-IT200 (LA) scanning electron microscope

Table 1. Cooking quality of rice varieties with different eating qualities and their response to nitrogen fertiliser rates

Year	Cultivar	Treatment	Amylose content (%)	Gel consistency (mm)	Alkali spreading value	Protein content (%)
2023	Xudao 3	N0	21.41^{a}	73.27^{e}	8.56^{d}	7.74^{d}
		N1	20.25^{b}	76.08^{d}	8.02^{e}	7.78^{d}
		N2	18.38^{c}	80.74^{b}	7.60^{g}	8.45^{c}
		N3	19.00^{c}	79.87^{b}	7.76^{f}	9.91^{a}
		mean	19.76	77.49	7.99	8.47
	Zhengdao C42	N0	18.86^{c}	78.88^{bc}	9.60^{a}	6.99^{f}
		N1	16.43^{d}	80.37^{b}	9.23^{b}	7.38^{e}
		N2	15.08^{e}	83.36^{a}	8.49^{d}	8.58^{c}
		N3	16.15^{d}	77.42^{cd}	8.79^{c}	9.56^{b}
		mean	16.63	80.01	9.03	8.13
2024	Huageng 9	N0	20.76^{a}	55.72^{f}	8.27^{b}	7.43^{c}
		N1	18.25^{b}	60.33^{e}	7.43^{d}	7.80^{b}
		N2	16.82^{c}	68.19^{d}	6.93^{f}	8.21^{a}
		N3	17.33^{c}	67.34^{d}	7.08^{ef}	8.38^{a}
		mean	18.29	62.90	7.43	7.96
	Nangeng 9308	N0	15.31^{d}	65.83^{d}	8.77^{a}	6.48^{e}
		N1	14.74^{d}	74.57^{c}	7.80^{c}	6.80^{d}
		N2	11.86^{f}	86.90^{a}	7.15^{e}	6.91^{d}
		N3	12.75^{e}	83.55^{b}	7.20^{e}	7.33^{c}
		mean	13.67	77.71	7.73	6.88
ANOVA						
Year (Y)			296.33**	540.27**	1 051.14**	661.55**
Cultivar (C)			906.67**	569.11**	555.35**	430.73**
Nitrogen fertiliser rate (N)			142.77**	187.51**	382.60**	448.25**
Y × C			33.77**	286.41**	165.77**	115.00**
Y × N			ns	60.28**	19.64**	113.60**
C × N			ns	5.16**	4.67**	ns
Y × C × N			6.64**	19.11**	ns	14.32**

Xudao 3 and Huageng 9 represent rice cultivars with moderate eating quality; Zhengdao C42 and Nangeng 9308 represent those with superior eating quality, respectively. N0 – no nitrogen application; N1 – 0.59 g N/pot; N2 – 1.18 g N/pot; N3 – 1.76 g N/pot. Values followed by different letters indicate statistical significance at $P < 0.05$ within the same column and year. Significance difference of F-values at $^{*}P < 0.05$ and $^{**}P < 0.01$; ns – not significant difference

https://doi.org/10.17221/20/2026-PSE

Table 2. Differences in root anatomy of rice with differing eating qualities, and their response to nitrogen application at the initial panicle differentiation stage

Year	Cultivar	Treatment	CCA	CLCA	SD	RD	PLCA
			(× $10^4 \mu m^2$)		(μm)		(%)
2023	Xudao 3	N0	48.35^{d}	34.31^{d}	150.19^{b}	782.69^{d}	74.76^{d}
		N1	64.30^{c}	54.41^{b}	160.77^{a}	903.42^{c}	81.17^{bc}
		N2	107.59^{a}	72.80^{a}	170.25^{a}	$1\,170.39^{a}$	81.82^{bc}
		N3	75.48^{b}	71.29^{a}	165.38^{a}	980.05^{b}	85.73^{b}
		mean	73.93	58.20	161.65	714.13	80.87
	Zhengdao C42	N0	28.01^{e}	23.23^{e}	139.56^{c}	597.30^{e}	78.74^{c}
		N1	46.76^{d}	40.11^{cd}	164.37^{a}	771.56^{d}	86.95^{b}
		N2	52.30^{d}	40.77^{c}	166.97^{a}	816.08^{d}	92.99^{a}
		N3	53.16^{d}	38.14^{cd}	164.89^{a}	822.52^{d}	85.60^{b}
		mean	45.06	35.57	158.95	751.87	86.07
2024	Huageng 9	N0	58.68^{cd}	52.81^{cd}	162.12^{c}	830.56^{c}	89.98^{d}
		N1	65.90^{abc}	60.98^{abc}	170.02^{c}	903.43^{bc}	92.50^{bc}
		N2	73.37^{a}	68.60^{a}	185.73^{b}	$1\,072.87^{a}$	93.49^{ab}
		N3	70.61^{ab}	65.78^{ab}	193.25^{b}	$1\,054.68^{a}$	92.93^{bc}
		mean	67.14	62.04	177.78	965.39	92.23
	Nangeng 9308	N0	51.81^{d}	47.71^{d}	159.55^{c}	742.18^{d}	92.02^{c}
		N1	62.12^{bc}	58.04^{bc}	166.99^{c}	832.30^{c}	93.21^{ab}
		N2	63.06^{bc}	59.25^{bc}	184.56^{b}	911.57^{b}	94.11^{a}
		N3	62.67^{bc}	56.88^{c}	216.61^{a}	865.39^{bc}	90.78^{d}
		mean	59.92	55.47	181.93	837.86	92.53
ANOVA							
Year (Y)			7.19^{*}	106.98^{**}	131.8^{**}	15.04^{**}	197.05^{**}
Cultivar (C)			143.98^{**}	161.91^{**}	ns	198.08^{**}	18.82^{**}
Nitrogen fertiliser rate (N)			58.29^{**}	66.07^{**}	65.83^{**}	85.12^{**}	19.80^{**}
Y × C			51.75^{**}	48.99^{**}	ns	11.24^{**}	14.89^{**}
Y × N			16.24^{**}	9.03^{**}	18.60^{**}	3.04^{*}	8.47^{**}
C × N			11.06^{**}	9.90^{**}	5.38^{**}	7.94^{**}	5.64^{**}
Y × C × N			6.69^{**}	3.71^{*}	3.97^{*}	3.82^{*}	2.95^{*}

Xudao 3 and Huageng 9 represent rice cultivars with moderate eating quality; Zhengdao C42 and Nangeng 9308 represent those with superior eating quality, respectively. N0 – no nitrogen application; N1 – 0.59 g N/pot; N2 – 1.18 g N/pot; N3 – 1.76 g N/pot. Values followed by different letters indicate statistical significance at $P < 0.05$ within the same column and year. Significance difference of F-values at $^{*}P < 0.05$ and $^{**}P < 0.01$; ns – not significant difference; CCA – cortical cell area; CLCA – cortical living cell area; SD – stele diameter; RD – root diameter; PLCA – proportion of cortical living area

(SEM). The acquired images were analysed with ImageJ software (version 1.8.0; National Institutes of Health, Bethesda, USA) to quantify the aerenchyma area, cortical cell area, stele diameter, and stele diameter to root diameter. The proportions of living cell area to cortical cell area, aerenchyma area to cortical cell area, and stele diameter to root diameter were further calculated. Each treatment included six independent biological replicates. The reagents employed were as follows: 2.5% (*v*/*v*) glutaraldehyde for fixation, 0.1 mol/L phosphate buffer (pH 7.4) for sample rinsing, and gradient concentrations of ethanol for dehydration.

The formulas for result calculation are as follows:

$$\text{aerenchyma proportion (\%)} = [\text{aerenchyma area } (\mu m^2)/\text{cortical area } (\mu m^2)] \times 100;$$

cortical living cell area (μm^2) = cortical area (μm^2) – aerenchyma area (μm^2);
cortical living cell proportion (%) = [cortical living cell area (μm^2)/cortical area (μm^2)] × 100;
stele-to-root diameter ratio = stele diameter (μm)/root diameter (μm).

Data analysis. Statistical analysis was conducted using analysis of variance (ANOVA) in SPSS statistical analysis software (version 27.0; IBM Corp., Armonk, USA). Means were tested by the least significant difference (*LSD*) test at $P < 0.05$. Line and bar charts were generated with Origin 2025 (OriginLab Corporation, Northampton, USA). Scanning electron microscope (SEM) images were analysed with ImageJ software (version 1.8.0; National Institutes of Health, Bethesda, USA).

RESULTS

Grain cooking quality. Results from two consecutive years indicated that rice variety, nitrogen application rate, and their interaction significantly affected indices of rice cooking quality ($P < 0.05$; Table 1). With increasing nitrogen application rate, the amylose content and alkali spreading value of the four tested rice varieties exhibited a decreasing-then-increasing trend, with minimum values consistently recorded at the N2 level. In contrast, gel consistency showed a reverse increasing-then-decreasing trend, peaking at the N2 level. Grain protein content was elevated in response to higher nitrogen application rates. Specifically, compared with N0, amylose

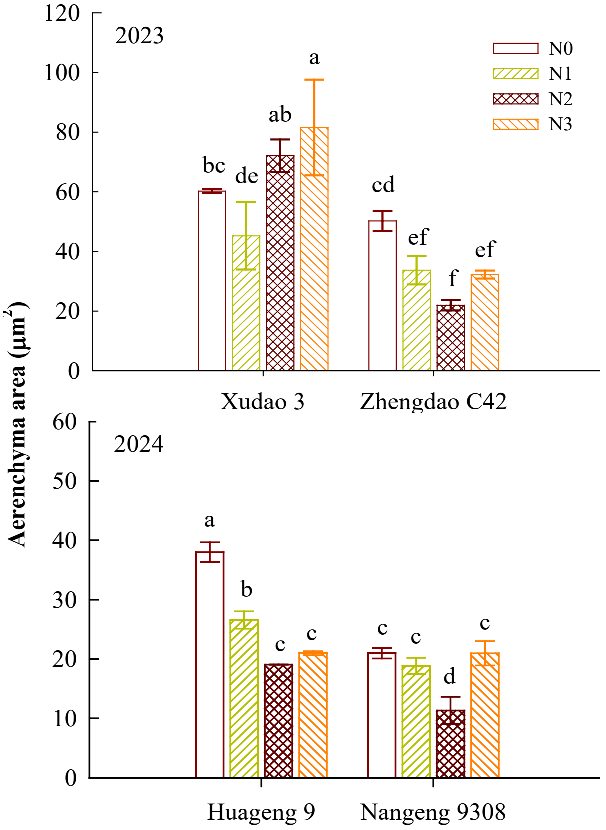

Figure 1. Differences in root aerenchyma area of rice with differing eating qualities, and their response to nitrogen application at the initial panicle differentiation stage. Xudao 3 and Huageng 9 represent rice cultivars with moderate eating quality; Zhengdao C42 and Nangeng 9308 represent those with superior eating quality, respectively. N0 – no nitrogen application; N1 – 0.59 g N/pot; N2 – 1.18 g N/pot; N3 – 1.76 g N/pot. Vertical bars represent ≈ standard error of the mean. Different letters of the column indicate statistical significance at $P < 0.05$ within the same stage and the same year

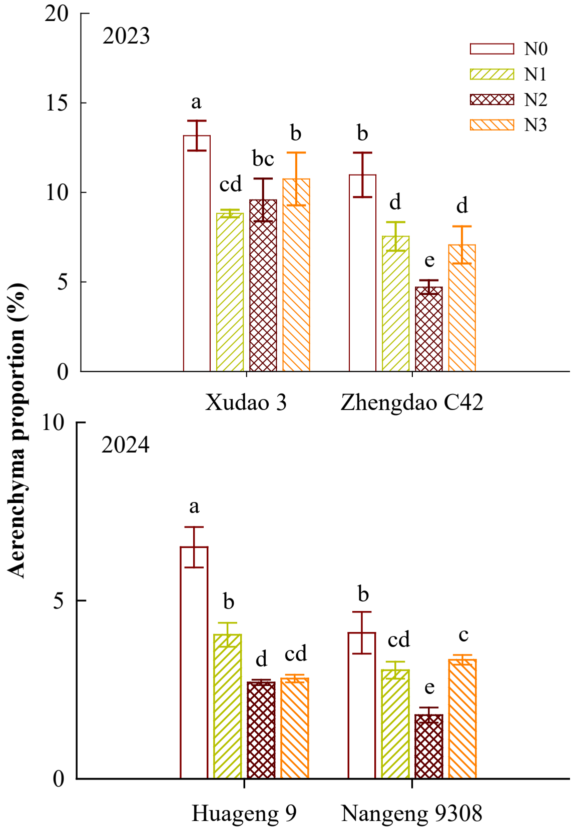

Figure 2. Differences in root aerenchyma proportion of rice with differing eating qualities, and their response to nitrogen application at the initial panicle differentiation stage. Xudao 3 and Huageng 9 represent rice cultivars with moderate eating quality; Zhengdao C42 and Nangeng 9308 represent those with superior eating quality, respectively. N0 – no nitrogen application; N1 – 0.59 g N/pot; N2 – 1.18 g N/pot; N3 – 1.76 g N/pot. Vertical bars represent ≈ standard error of the mean. Different letters of the column indicate statistical significance at $P < 0.05$ within the same stage and the same year

content in Huageng 9 and Nangeng 9308 at the N2 level decreased by 18.98–22.53% in 2024, while their alkali spreading value declined by 16.20–18.47% in the same year. Gel consistency, however, was significantly increased by 22.38% to 32.01% in 2024.

Under the same nitrogen application level, significant differences in cooking quality were observed among varieties with distinct eating-quality attributes. Compared to Huageng 9 (moderate eating quality), Nangeng 9308 (superior eating quality) showed a 25.26% reduction in amylose content and a 13.57% reduction in protein content, along with a 23.55% increase in gel consistency and a 4.04% increase in alkali spreading value. The two-year experimental results showed good consistency. Overall, the analysis indicated that the cooking quality of superior-eating-quality varieties (Zhengdao C42, Nangeng 9308) was significantly better than that of moderate-eating-quality varieties (Xudao 3, Huageng 9).

Root anatomical structure. Rice variety, nitrogen application rate, and their interaction significantly influenced root anatomical traits in both experimental years, including cortical cell area, cortical living cell area, stele diameter, root diameter, and the proportion of living cells ($P < 0.05$; Table 2). Increasing the nitrogen application rate generally promoted these traits, with the cortical area, living cortical cell area, stele diameter, root diameter, and living cell proportion all being significantly elevated. These parameters typically reached their maximum values under the N2 or N3 treatments, a pattern consistent across both years. Under the same nitrogen level, superior-eating-quality cultivars exhibited distinct anatomical profiles. Specifically, Nangeng 9308 showed a 10.75% reduction in cortical cell area and a10.59% reduction in living cortical cell area relative to Huageng 9, while its living cell proportion increased by an average of 0.28%. Similarly, Zhengdao C42 displayed substantial reductions of 39.05% in cortical cell area and 38.88% in living cortical cell area compared to Xudao 3, alongside a notable average increase of 6.43% in living cell proportion.

In contrast to the proportion of living cells, both the area and proportion of root aerenchyma followed a V-shaped trend with increasing nitrogen application rate, reaching minima at the N2 level, except for Xudao 3 (Figures 1 and 2). Compared with the N0 treatment, the aerenchyma area and proportion at the N2 level were reduced by 49.84% and 58.40% in Huageng 9, and by 46.04% and 56.48% in Nangeng 9308, respectively. At the same nitrogen level, Nangeng 9308 showed average reductions of 31.09% and 23.57% in aerenchyma area and proportion, respectively, relative to Huageng 9. This response trend was consistent across the 2023 and 2024 growing seasons. In summary, the superior eating-quality cultivars exhibited the smallest root aerenchyma areas and proportion under the N2 treatment.

The stele-to-root diameter ratio (SD/RD) decreased generally with increasing nitrogen application, although the differences among rates were relatively small (Figure 3). Under the same nitrogen level, the superior-eating-quality cultivars (Nangeng 9308 and Zhengdao C42) showed significantly higher SD/RD than the moderate-eating-quality cultivars (Huageng 9 and Xudao 3), with average increases of 16.91% and 22.36%, respectively.

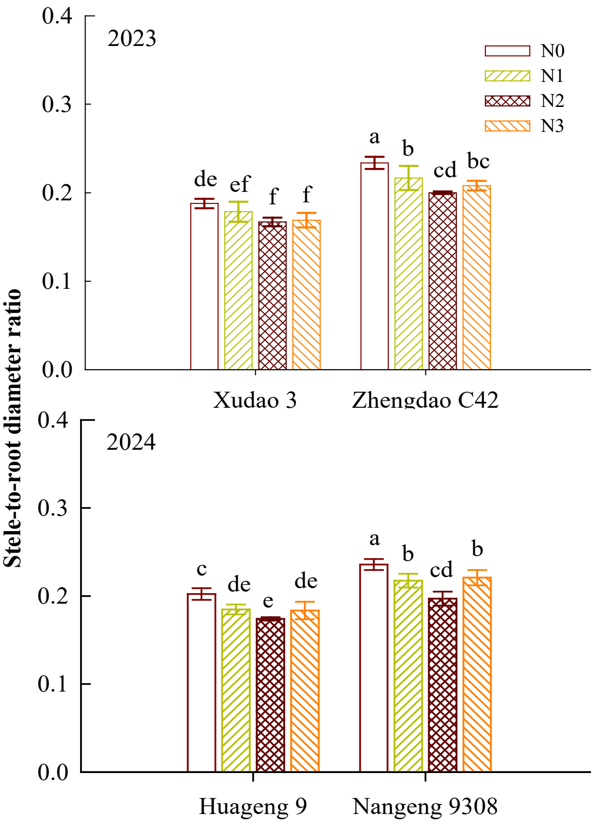

Figure 3. Differences in root stele-to-root diameter ratio (SD/RD) of rice under different eating qualities and nitrogen application rates at the initial panicle differentiation stage. Xudao 3 and Huageng 9 represent rice cultivars with moderate eating quality; Zhengdao C42 and Nangeng 9308 represent those with superior eating quality, respectively. N0 – no nitrogen application; N1 – 0.59 g N/pot; N2 – 1.18 g N/pot; N3 – 1.76 g N/pot. Vertical bars represent ≈ standard error of the mean. Different letters of the column indicate statistical significance at $P < 0.05$ within the same stage and the same year

Root senescence characteristics. Root SOD activity varied significantly among cultivars and in response to nitrogen application. It generally exhibited an initial increase followed by a decrease during the growth period, peaking at the heading stage (Figure 4). As the nitrogen application rate increased, root SOD activity reached its maximum at the N2 level. At this optimal nitrogen level during heading, root SOD activ-

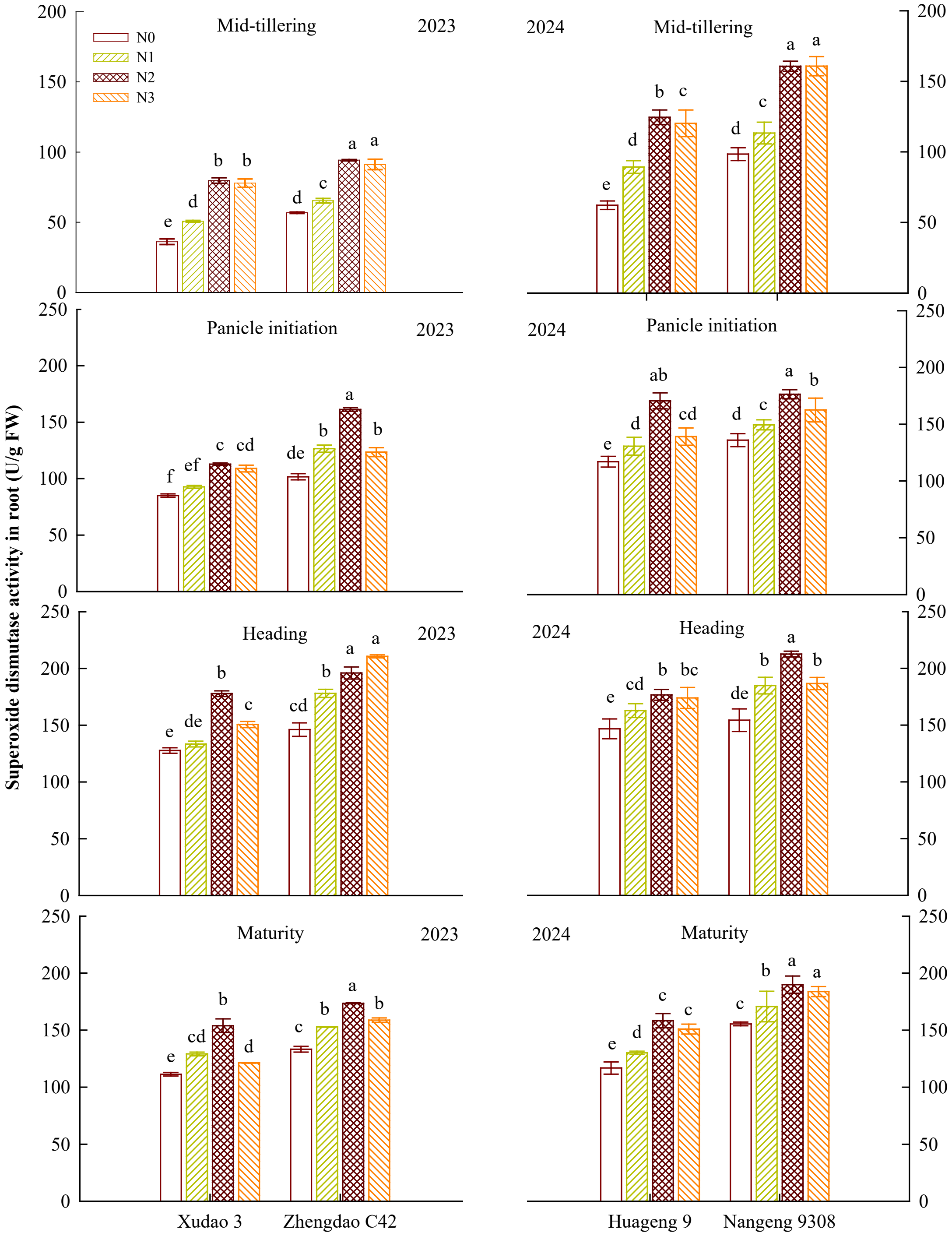

Figure 4. Superoxide dismutase (SOD) activity of rice under varied eating qualities and nitrogen application rates. Xudao 3 and Huageng 9 represent rice cultivars with moderate eating quality; Zhengdao C42 and Nangeng 9308 represent those with superior eating quality, respectively. N0 – no nitrogen application; N1 – 0.59 g N/pot; N2 – 1.18 g N/pot; N3 – 1.76 g N/pot. Vertical bars represent ≈ standard error of the mean. Different letters of the column indicate statistical significance at $P < 0.05$ within the same stage and the same year. FW – fresh weight

https://doi.org/10.17221/20/2026-PSE

ity increased by 20.46% in Huageng 9 and by 37.70% in Nangeng 9308 compared with the N0 treatment. Under the same nitrogen level, Nangeng 9308 maintained an average of 11.87% higher SOD activity than Huageng 9. This trend was consistent across the 2023 and 2024 growing seasons. Collectively, root SOD activity peaked at the N2 level across all varieties, with the highest values consistently observed in superior eating-quality cultivars.

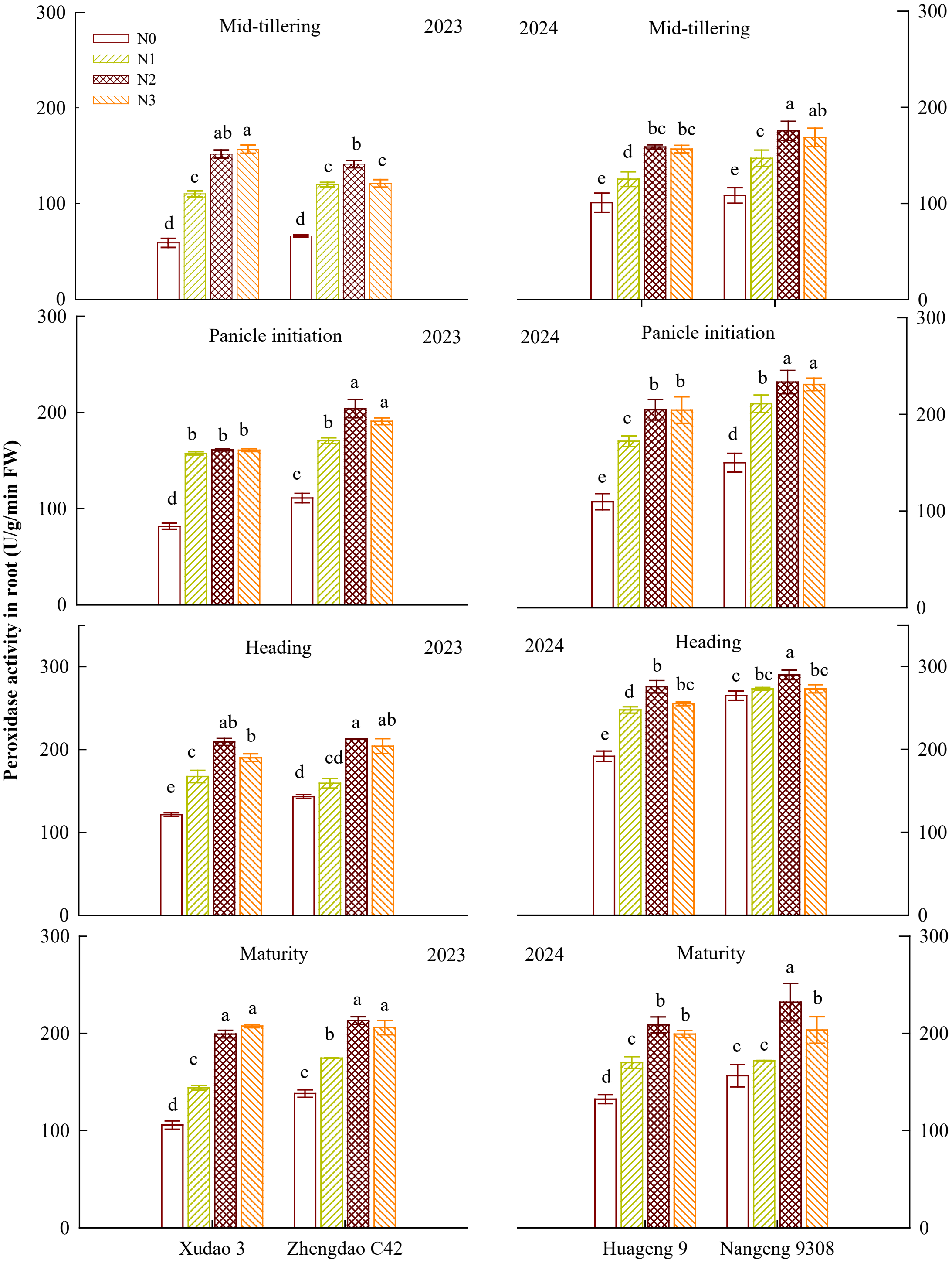

Figure 5. Peroxidase (POD) activity of rice under varied eating qualities and nitrogen application rates. Xudao 3 and Huageng 9 represent rice cultivars with moderate eating quality; Zhengdao C42 and Nangeng 9308 represent those with superior eating quality, respectively. N0 – no nitrogen application; N1 – 0.59 g N/pot; N2 – 1.18 g N/pot; N3 – 1.76 g N/pot. Vertical bars represent ≈ standard error of the mean. Different letters of the column indicate statistical significance at $P < 0.05$ within the same stage and the same year. FW – fresh weight

Similar to root SOD activity, root POD activity exhibited a unimodal pattern during the growth cycle, increasing initially before declining after reaching a peak at the heading stage (Figure 5). As nitrogen application rates increased, root POD activity peaked under the N2 treatment, a trend that was consistent across both experimental years. Compared with the N0 treatment, root POD activity at the heading stage

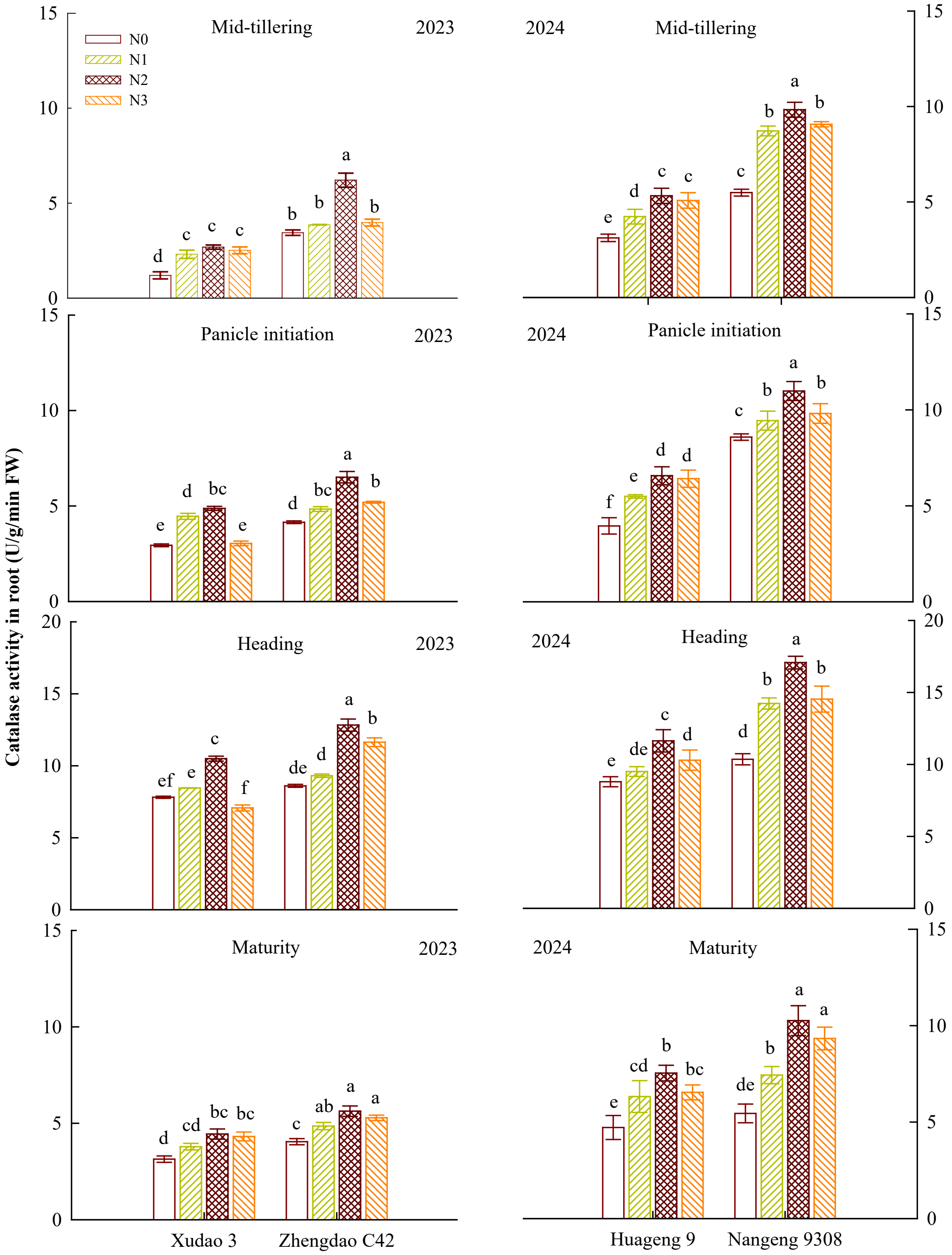

Figure 6. Catalase (CAT) activity of rice under varied eating qualities and nitrogen application rates. Xudao 3 and Huageng 9 represent rice cultivars with moderate eating quality; Zhengdao C42 and Nangeng 9308 represent those with superior eating quality, respectively. N0 – no nitrogen application; N1 – 0.59 g N/pot; N2 – 1.18 g N/pot; N3 – 1.76 g N/pot. Vertical bars represent ≈ standard error of the mean. Different letters of the column indicate statistical significance at $P < 0.05$ within the same stage and the same year. FW – fresh weight

increased by 43.81% in Huageng 9 and by 9.43% in Nangeng 9308. Under the same nitrogen level, the POD activity in Nangeng 9308 and Zhengdao C42 was on average 13.50% and 4.50% higher than that in Huageng 9 and Xudao 3, respectively. The results indicate that across all varieties, root POD activity

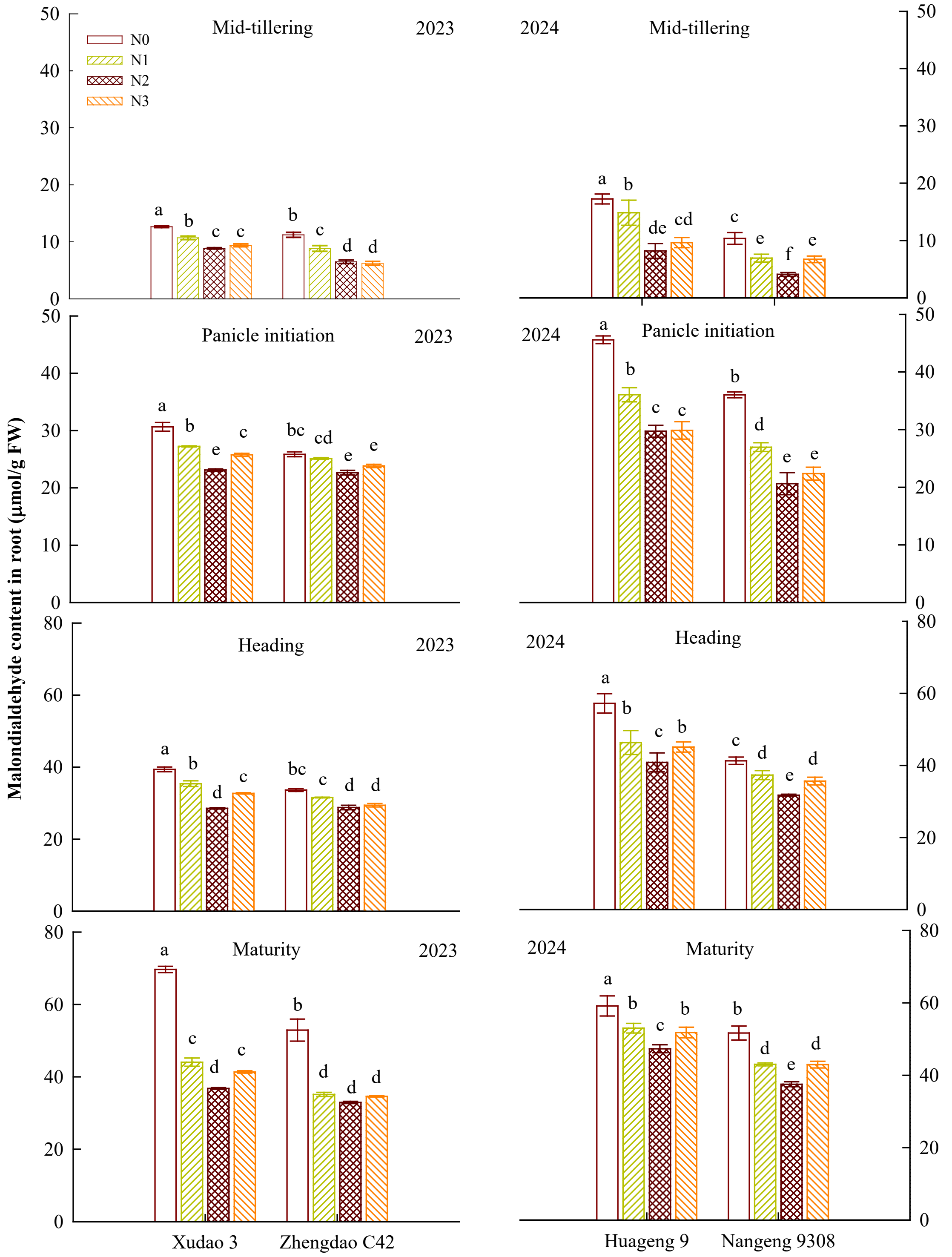

Figure 7. Malondialdehyde (MDA) content of rice under varied eating qualities under nitrogen application rates. Xudao 3 and Huageng 9 represent rice cultivars with moderate eating quality; Zhengdao C42 and Nangeng 9308 represent those with superior eating quality, respectively. N0 – no nitrogen application; N1 – 0.59 g N/pot; N2 – 1.18 g N/pot; N3 – 1.76 g N/pot. Vertical bars represent ≈ standard error of the mean. Different letters of the column indicate statistical significance at $P < 0.05$ within the same stage and the same year. FW – fresh weight

https://doi.org/10.17221/20/2026-PSE

peaked under the N2 treatment, with the highest values consistently observed in superior eating-quality cultivars.

Similar to root POD activity, root CAT activity also fluctuated throughout the growth cycle, reaching its maximum at the heading stage (Figure 6). With increasing nitrogen application rates, it reached a maximum at the N2 level – a trend consistent across both experimental years. Compared with the N0 treatment, root CAT activity at the heading stage increased by 32.31% in Huageng 9 and by 64.83% in Nangeng 9308 under the N2 treatment. At the same nitrogen level, Nangeng 9308 exhibited 39.69% higher root CAT activity than Huageng 9, and Zhengdao C42 showed a 25.25% greater activity than Xudao 3. Overall, across all varieties, root CAT activity peaked under the N2 treatment, with the highest values consistently observed in superior-eating-quality cultivars.

In contrast to root CAT activity, root MDA content exhibited a distinct "decrease-then-increase" trend, with its lowest value observed under the N2 treatment (Figure 7). At the heading stage, MDA content decreased by 28.61% in Huageng 9 and 23.12% in Nangeng 9308 under N2 treatment compared with N0. The result was consistent across the 2023 and 2024 trials. Under the same nitrogen level, MDA levels in Nangeng 9308 and Zhengdao C42 were both 22.97% and 9.26% lower than those in Huageng 9 and Xudao 3, respectively. The results indicate that superior eating-quality cultivars accumulated significantly less root MDA under the N2 treatment.

Photosynthetic rate in leaves. Photosynthetic rate varied significantly among cultivars and in response to nitrogen application (Figure 8). As the nitrogen application rate increased, the photosynthetic rate reached its maximum at the N2 level. At this optimal nitrogen level during heading, photosynthetic rate increased by 18.8% in Huageng 9 and by 35.7% in Nangeng 9308 compared with the N0 treatment. Under the same nitrogen level, Nangeng 9308 maintained an average of 13.87% higher photosynthetic rate than Huageng 9. This trend was consistent across the 2023 and 2024 growing seasons.

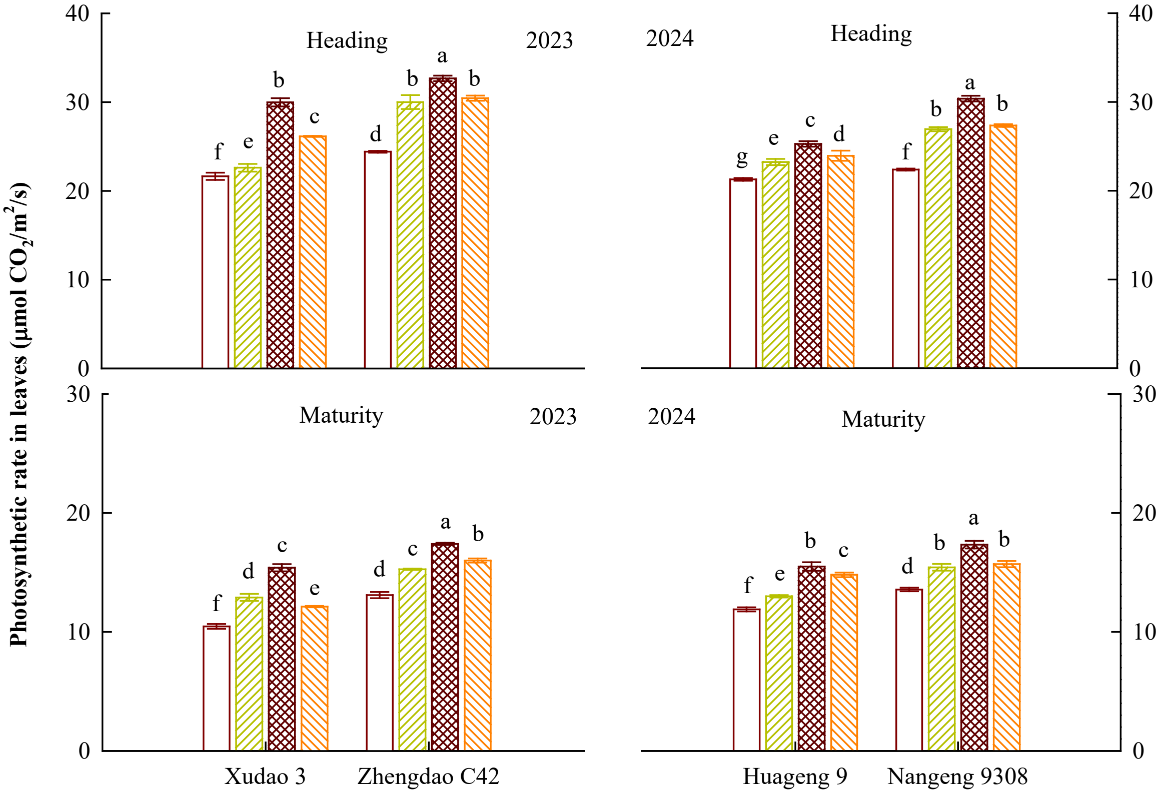

Figure 8. Photosynthetic rate (P_n) under varied eating qualities under nitrogen application rates. Xudao 3 and Huageng 9 represent rice cultivars with moderate eating quality; Zhengdao C42 and Nangeng 9308 represent those with superior eating quality, respectively. N0 – no nitrogen application; N1 – 0.59 g N/pot; N2 – 1.18 g N/pot; N3 – 1.76 g N/pot. Vertical bars represent ≈ standard error of the mean. Different letters of the column indicate statistical significance at $P < 0.05$ within the same stage and the same year

Relationship between rice root anatomical structure and physiological activities. A significant correlation was observed between rice root anatomical structure and root senescence (Figure 9). Correlation analysis indicated that both root aerenchyma area and its proportion were highly significantly negatively correlated with the activities of SOD, POD, CAT, and photosynthetic rate (P_n), while showing a highly significant positive correlation with MDA content. Conversely, the stele diameter and the proportion of cortical living cells demonstrated significant to highly significant positive correlations with Pn, SOD, POD, and CAT activities, and significant to highly significant negative correlations with MDA content.

Relationship between root physiological activity, anatomical structure and grain cooking quality. Correlation analysis (Figure 10) revealed that root antioxidant enzyme (SOD, POD, CAT) activities, P_n, stele diameter, and cortical living cell proportion were significantly negatively correlated with grain amylose content but positively correlated with gel consistency. In contrast, root MDA content, aerenchyma area, and aerenchyma proportion were significantly higher and positively correlated with amylose content, whereas they were negatively correlated with gel consistency.

DISCUSSION

Cooking quality of rice varieties with distinct eating qualities and their responses to nitrogen. Rice quality is primarily determined by varietal genetics but is also strongly influenced by agronomic management (Shi et al. 2022, Chen et al. 2024, Li et al. 2025). Amylose content and gel consistency are pivotal determinants of cooking quality. Reduced levels of protein and amylose contribute to a softer texture, thereby enhancing palatability, while lower gel consistency is associated with increased coarseness and diminished cooking quality (Bahmaniar et al. 2007, Li et al. 2025). Our results indicate that the cooking quality of varieties with differing palatability initially improved but subsequently declined with increasing nitrogen application. Compared to N0 treatment, N fertilisation significantly reduced amylose content. Gel consistency first increased and

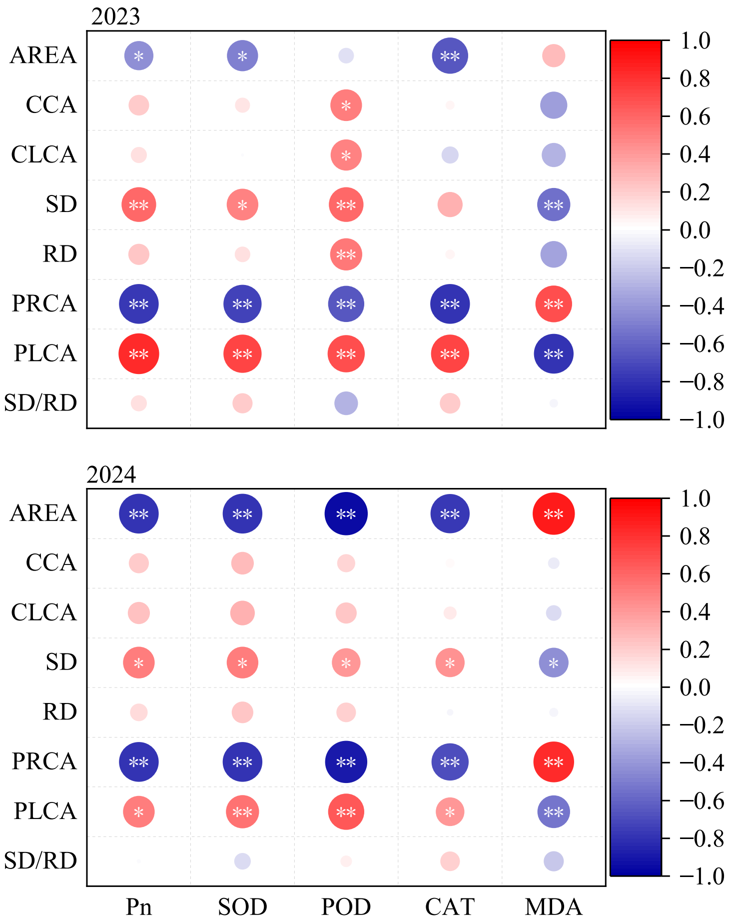

Figure 9. Relationship between root physiological activity and root anatomical structure of rice. *F*-values significance at **P* < 0.05 and ***P* < 0.01; ns – not significant at *P* = 0.05; AREA – aerenchyma area; CCA – cortical cell area; CLCA – cortical living cell area; SD – stele diameter; RD – root diameter; PRCA – aerenchyma proportion; PLCA – proportion of cortical living cell area; SD/RD – stele-to-root diameter ratio; P_n – photosynthetic rate; SOD – superoxide dismutase; POD – peroxidase; CAT – catalase; MDA – malondialdehyde

https://doi.org/10.17221/20/2026-PSE

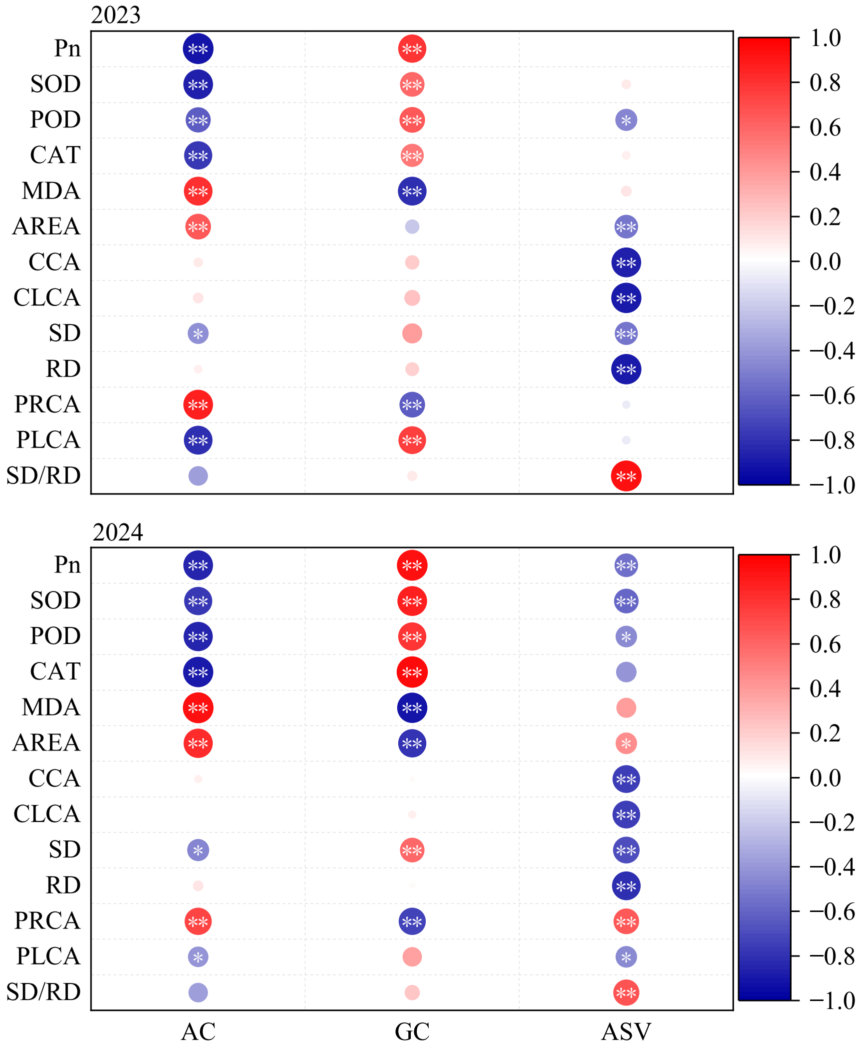

Figure 10. Relationships between root physiological activity, root anatomical structure and eating quality of rice. *F*-values significance at $^{*}P < 0.05$ and $^{**}P < 0.01$; ns – not significant at $P = 0.05$; P_n – photosynthetic rate; SOD – superoxide dismutase; POD – peroxidase; CAT – catalase; MDA – malondialdehyde; AREA – aerenchyma area; CCA – cortical cell area; CLCA – cortical living cell area; SD – stele diameter; RD – root diameter; PRCA – aerenchyma proportion; PLCA – proportion of cortical living cell area; SD/RD – stele-to-root diameter ratio; AC – amylose content; GC – gel consistency; ASV – alkaline spreading value

then decreased, whereas the alkali spreading value exhibited an opposite trend (Table 1). These findings align with Zhu et al. (2016), who reported that moderate N application could reconcile high yield with superior cooking quality. Furthermore, supporting our observations, Zhang et al. (2021) demonstrated that moderate N application improves processing, appearance, and cooking qualities in mid-season indica rice by prolonging the grain-filling period and increasing the filling rate, thereby raising grain weight. However, excessive nitrogen application (N3) led to a rebound in amylose content, which can be attributed to differences in genetic thresholds for nitrogen response among varieties. When nitrogen supply exceeds the optimal level, it disrupts the carbon-nitrogen metabolic balance, thereby diverting substrates from starch accumulation to protein synthesis and negatively impacting rice cooking quality – a mechanism well documented in previous studies (Kusano et al. 2011, Liu et al. 2024, Liu et al. 2025, Xu et al. 2025).

Notable variational differences in rice quality exist. Studies on semi-glutinous japonica rice indicate that superior eating-quality varieties possess superior cooking quality, characterised by lower protein content and more favourable viscosity profiles (Liu et al. 2022), highlighting their intrinsic quality advantages. Consistently, our study found that superior eating-quality varieties generally outperformed ordinary ones in cooking quality (Table 1). This superiority can be traced to their lower GBSSI (granule-bound starch synthase I) activity, which results in a higher proportion of amylopectin with shorter branch chains, yielding a soft and cohesive texture. Moreover, their typically lower protein content facilitates the formation of a porous structure during cooking, enhancing water absorption and improving the fluffiness, stickiness, and elasticity of the cooked rice (Wang et al. 2025, Ma et al. 2025).

https://doi.org/10.17221/20/2026-PSE

Differences in root anatomical structure of rice varieties with distinct eating qualities and their responses to nitrogen fertiliser regulation. Water and nutrients absorbed by the roots move inward through the epidermis. They are transported toward the stele *via* apoplastic and symplastic pathways (Figure 11), ultimately supplying the shoots – a process intrinsically linked to root anatomy (Zhang et al. 2020, Lynch et al. 2023, Srivastava et al. 2025) (Figure 12). While studies suggest that structural features such as fewer cortical cell layers, reduced aerenchyma area, and a higher stele-to-root diameter ratio can enhance water and nutrient uptake, thereby supporting high yield and cooking quality in rice (De Bauw et al. 2019, Li et al. 2022, Eweda et al. 2025), other findings indicate a different mechanism in modern varieties. Fonta et al. (2022) propose that high NH_4^+ uptake and nitrogen accumulation may correlate more strongly with larger root diameter, greater cortical and stele area, and increased number of xylem vessels, rather than with reduced aerenchyma size. In this study, the area and proportion of root aerenchyma at panicle initiation exhibited a V-shaped pattern in response to increasing nitrogen supply, initially decreasing, then increasing (Figures 1–2). The larger aerenchyma area under the N0 treatment reflects an adaptive response to nitrogen deficiency, driven physiologically by programmed cell death in cortical cells triggered by nitrogen starvation – a mechanism consistent with reports that various stresses induce aerenchyma formation (York et al. 2015, Zhen et al. 2020, Lynch et al. 2023). The optimal N rate (N2) alleviated such stress and suppressed excessive aerenchyma development. Notably, overdeveloped aerenchyma can hinder root growth by accelerating programmed cell death and reducing the population of functional cortical cells, thereby impairing nitrogen uptake and, ultimately, grain yield and cooking quality (Liu et al. 2023, Eweda et al. 2025). The present results indicated that stele and adventitious root diameters generally increased, then decreased, with N rate, peaking at N2 (Table 2). A plausible mechanism is that larger root and stele diameters and more xylem vessels enhance N uptake and transport (Li et al. 2022). A wider stele shortens water transport distance, raising hydraulic conductance and absorption; thicker adventitious roots expand soil contact, compensating for fewer roots and improving nutrient capture (Schneider et al. 2017, Drobnitch et al. 2025). These changes collectively promote grain filling and the development of cooking quality. Excessive nitrogen or nitrogen

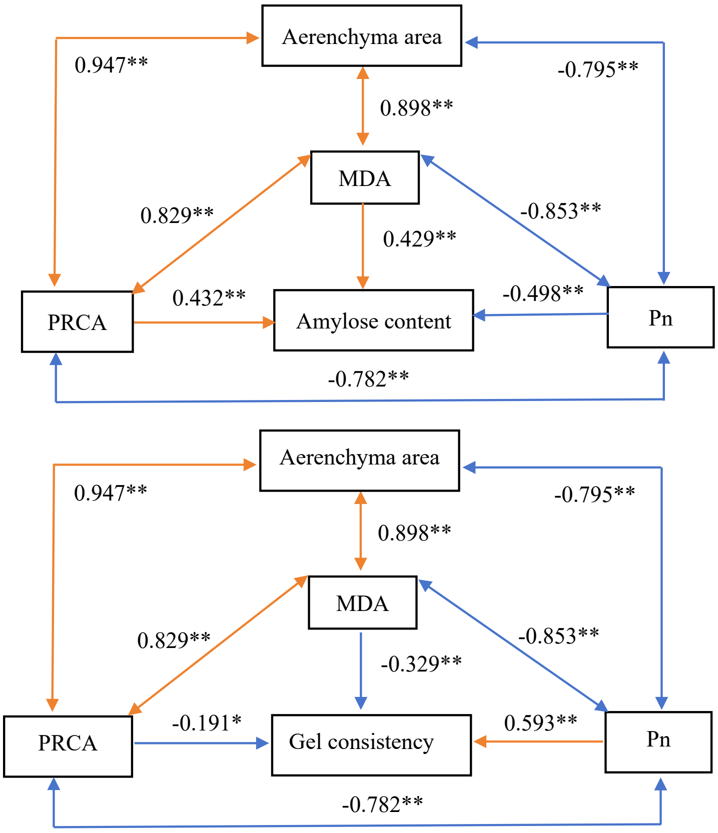

Figure 11. Path analysis of root traits and photosynthetic rate on rice cooking quality. PRCA – aerenchyma proportion; P_n – photosynthetic rate

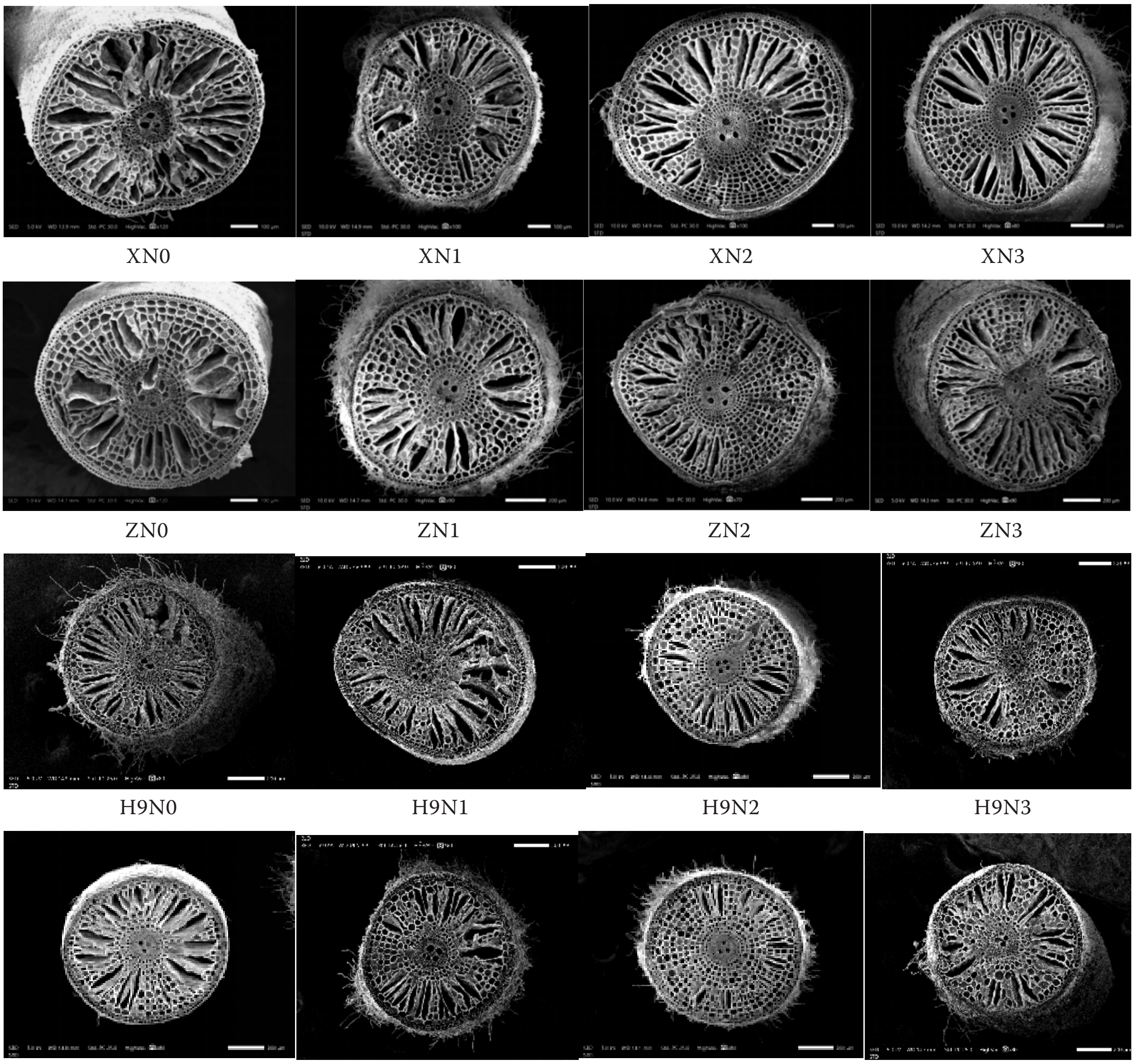

XN0 XN1 XN2 XN3

ZN0 ZN1 ZN2 ZN3

H9N0 H9N1 H9N2 H9N3

NN0 NN1 NN2 NN3

Figure 12. Differences in root anatomy of rice with differing eating qualities, and their response to nitrogen application at the initial panicle differentiation stage. Xudao 3 and Huageng 9 represent rice cultivars with moderate eating quality; Zhengdao C42 and Nangeng 9308 represent those with superior eating quality, respectively. N0 – no nitrogen application; N1 – 0.59 g N/pot; N2 – 1.18 g N/pot; N3 – 1.76 g N/pot

deficiency will disrupt the root "flow" function, leading to an imbalance in "source-sink-flow" and, thus, deterioration of cooking quality.

This study demonstrated that superior eating-quality cultivars had lower aerenchyma area and proportion than ordinary cultivars (Figures 1–2). An increase in aerenchyma area reduces both the number and area of living cortical cells, thereby inhibiting symplastic transport of water and nutrients. Moreover, the random distribution of aerenchyma in the cortex reduces cortical cell numbers, thereby reducing intercellular transport routes and creating more tortuous pathways for nutrient and water movement (Salah et al. 2022, Guo et al. 2024, Chen et al. 2024). In contrast, the superior eating-quality cultivars here exhibited a higher proportion of living cells (Table 2). A greater population of living cortical cells establishes more channels for nutrient and water transport, thus facilitating their movement (Liu et al. 2023). Furthermore, a larger stele-to-root diameter ratio and more xylem vessels enhance nutrient and water transport to the shoots, thereby promoting shoot growth and contributing to the formation of grain cooking quality (Liu et al. 2023, Guo et al. 2024, Chen et al. 2024). Thus, cortical area, root and stele diameter, and xylem vessel number govern the efficiency of nutrient and water transport from roots to shoots – reinforcing the "flow" – which ensures sufficient substrate supply for leaf photosynthesis and sustains high photosynthetic capacity – stabilising the "source" – thereby promoting grain filling and enhancing cooking quality (Table 2, Figure 8). The observed anatomical differences in superior eating-quality cultivars likely have a genetic basis. Elucidating this genetic architecture in future studies could identify key loci underlying these favourable root traits, providing valuable targets for marker-assisted selection in breeding programs aimed at concurrently improving root function and grain quality.

Differences in root physiological activity of rice with distinct eating quality and their response to nitrogen fertilisation. A well-established consequence of abiotic stress is ROS-mediated oxidative damage, which compromises root integrity and accelerates senescence (Lee and Masclaux-Daubresse 2021, Averill-Bates 2024, Tavu and Redillas 2025). To counteract this damage, plants upregulate key antioxidant enzymes, including SOD, POD, and CAT, to scavenge ROS and restore redox homeostasis (Zhen et al. 2020, Zhu et al. 2024, Tavu and Redillas 2025). The present results manifested that the highest antioxidant enzyme activities were observed under the N2 treatment (Figures 4–6). Our results align with those of Cui et al. (2025), who reported that optimal nitrogen application alleviates oxidative damage and lowers MDA content in roots. In contrast, excessive nitrogen suppresses antioxidant enzyme activities and elevates MDA levels (Cui et al. 2025). An appropriate nitrogen supply activates the antioxidant system, preserves the structural integrity of vascular and cortical tissues, delays senescence, and ultimately provides stable support for both source activity and flow efficiency during grain filling (Li et al. 2022, Zhang et al. 2025). Correlation analysis further supports these findings (Figure 9). Whereas nitrogen excess induces ion imbalance and metabolic stress, thereby aggravating oxidative damage and promoting programmed cell death (Liu et al. 2023, Qi et al. 2024, Tavu and Redillas 2025).

Notably, superior eating-quality rice varieties exhibited significantly stronger root antioxidant enzyme activities and lower MDA content than moderate-quality varieties (Figures 4–7), suggesting that superior eating-quality varieties can optimise antioxidant capacity under nitrogen fluctuation stress and sustain physiological vigour. In addition, enhanced antioxidant enzyme activity can alleviate oxidative stress, thereby suppressing abnormal programmed cell death in the cortex, reducing excessive aerenchyma formation, and maintaining a high proportion of living cells. This preservation of structural integrity prevents the disruption of root function caused by oxidative damage, thereby maintaining the roots' role as a source and ensuring unobstructed flow to the aboveground leaves for photosynthesis (Lopez-Valdivia et al. 2023, Salsinha et al. 2023, Meng et al. 2024, Ye et al. 2024). The results of the correlation analysis provide statistical support for this interpretation (Figure 9). Therefore, combining the selection of superior eating-quality varieties with rational nitrogen management can delay root senescence during late growth stages, ensure efficient nutrient uptake, optimise grain filling, and ultimately achieve synergistic improvements in both yield and cooking quality.

Relationship between root system characteristics and cooking quality across rice varieties with different eating quality. Root structural and functional traits play a crucial role in nutrient and water uptake, which, in turn, mediate shoot development and shape the final cooking quality of rice (Lv et al. 2022, Liu et al. 2023, Shiono et al. 2024, Li et al. 2025). The present results demonstrated that favourable root anatomical traits – a larger stele diameter, a higher proportion of viable cells, and reduced aerenchyma area and proportion – acted in concert with elevated antioxidant enzyme activities and photosynthetic rate to enhance rice cooking quality (Figure 10). Specifically, living-cell ratio and antioxidant activity were positively correlated with gel consistency and negatively correlated with amylose content in both 2023 and 2024 (Figure 10). A robust root structure helps maintain high antioxidant activity, delays senescence, ensures steady assimilate supply during grain filling, and thus improves cooking quality (Lv et al. 2022, Shiono et al. 2024). In contrast, excessive aerenchyma development compromises grain filling and cooking quality by reducing the number of living cortical cells, impairing water and nutrient transport, and diminishing antioxidant capacity, thereby accelerating root senescence (Liu et al. 2023, Chen et al. 2025). The stable "source" and smooth "flow" ensure a continuous and sufficient supply of photosynthate and nitrogen to the grain "sink", optimise the grain carbon-nitrogen metabolism balance, regulate the proper proportions of amylose and protein, and ultimately yield excellent cooking quality. In conclusion, an integrated breeding strategy for rice varieties with reduced aerenchyma formation and a high proportion of living cortical cells, coupled with practices such as balanced nitrogen fertilisation, enhances antioxidant capacity and photosynthetic rate, delays senescence, and ultimately enables the synergistic improvement of both grain yield and cooking quality.

By integrating root anatomical analysis with measurements of antioxidant enzyme activities and photosynthetic rate, this study provides novel insights into how root structural and functional characteristics mediate nitrogen's effects on cooking quality. Furthermore, the inclusion of protein content reinforces this mechanistic interpretation by linking root-mediated nitrogen uptake to compositional changes in the grain. Future studies should directly measure taste scores to validate the correlation between these cooking quality indicators and overall palatability under different N regimes. Additionally, given the inherent limitations of pot experiments, the applicability of these findings to field production and the consistency of results with pot experiments remain to be determined.

REFERENCES

Averill-Bates D. (2024): Reactive oxygen species and cell signalling. Review. Biochimica et Biophysica Acta (BBA)-Molecular Cell Research, 1871: 119573.

Bahmaniar M.A., Ranjbar G.A. (2007): Response of rice (*Oryza sativa* L.) cooking quality properties to nitrogen and potassium application. Pakistan Journal of Biological Sciences, 10: 1880–1884.

Bin Rahman A.R., Zhang J. (2023): Trends in rice research: 2030 and beyond. Food and Energy Security, 12: e390.

Bulas T., Schmidt B.R., Vorburger C., Fabian Y. (2025): Responses of rice paddy dragonflies to fertilisation in a mesocosm experiment. Agriculture, Ecosystems and Environment, 393: 109823.

Chen M., Chen G., Di D., Kronzucker H.J., Shi W. (2020): Higher nitrogen use efficiency (NUE) in hybrid "super rice" links to improved morphological and physiological traits in seedling roots. Journal of Plant Physiology, 251: 153191.

Chen Y., Ding Z., Yu T., Cao L., Duan Y., Zu Y., Li Z. (2024): Accumulation characteristics of heavy metals in three wild rice species and adaptation of root morphology and anatomical structure to native soil heavy metals in Yunnan. Ecological Indicators, 167: 112601.

Chen Z., Hou Y., Yan J., Cheng S., Wang Y., Feng G., Cai H. (2025): Comprehensive responses of root system architecture and anatomy to nitrogen stress in maize (Zea mays L.) genotypes with contrasting nitrogen efficiency. Agronomy, 15: 2083.

Chu G., Xu R., Chen S., Xu C., Liu Y., Abliz B., Zhang X., Wang D. (2022): Root morphological-physiological traits for japonica/indica hybrid rice with better yield performance under low N conditions. Food and Energy Security, 11: e355.

Cui Y., Ma W., Yang C., Bai Y., Xia T., Wei C., Zhang X., Zhou G. (2025): Subsurface drip irrigation combined with ammonium enhances root growth in rice (*Oryza sativa* L.), leading to improved N uptake and higher yield formation. Plants, 14: 891.

Dai L., Zhou X., Jian Z., Tian J., Li Y., Xu G. (2024): Comparison of leaf anatomical structure and photosynthetic characteristics between weedy rice and cultivated rice at the seedling stage. Scientific Reports, 14: 30829.

De Bauw P., Vandamme E., Lupembe A., Mwakasege L., Senthilkumar K., Dramé K.N., Merckx R. (2019): Anatomical root responses of rice to combined phosphorus and water stress–relations to tolerance and breeding opportunities. Functional Plant Biology, 46: 1009–1022.

Dou Z., Zhou Y., Zhang Y., Guo W., Xu Q., Gao H. (2024): Influence of nitrogen applications during grain-filling stage on rice (*Oryza sativa* L.) yield and grain quality under high temperature. Agronomy, 14: 216.

Drobnitch S.T., Donovan T.C., Wenz J.A., Flynn N.E., Schipanski M.E., Comas L.H. (2025): Can nitrogen availability impact plant performance under water stress? A review of traits, mechanisms, and whole plant effects. Plant and Soil, 511: 45–67.

Duan R., Lin Y., Yang L., Zhang Y., Hu W., Du Y., Huang M. (2023): Effects of antimony stress on growth, structure, enzyme activity and metabolism of Nipponbare rice (*Oryza sativa* L.) roots. Ecotoxicology and Environmental Safety, 249: 114409.

Eweda M.A., Jalil S., Rashwan A.K., Tsago Y., Hassan U., Jin X.J. (2025): Molecular and physiological characterizations of roots under drought stress in rice: a comprehensive review. Plant Physiology and Biochemistry, 225: 110012.

Firouzi S. (2015): Grain, milling, and head rice yields as affected by nitrogen rate and bio-fertilizer application. Acta Agriculturae Slovenica, 105: 241–248.

Fonta J.E., Giri J., Vejchasarn P., Lynch J.P., Brown K.M. (2022): Spatiotemporal responses of rice root architecture and anatomy to drought. Plant and Soil, 479: 443–444.

Fukagawa N.K., Ziska L.H. (2019): Rice: importance for global nutrition. Journal of Nutritional Science and Vitaminology, 65: S2–S3.

Galindo-Castañeda T., Lynch J.P., Six J., Hartmann M. (2022): Improving soil resource uptake by plants through capitalizing on synergies between root architecture and anatomy and root-associated microorganisms. Frontiers in Plant Science, 13: 827369.

Gharsallah C., Fakhfakh H., Grubb D., Gorsane F. (2016): Effect of salt stress on ion concentration, proline content, antioxidant enzyme activities and gene expression in tomato cultivars. AoB Plants, 8: plw055.

Guo Y., Du Y., Niu X., Ma Y., Song G., Cao C., Li P., Chen Y., Siddique K. (2024): Comparison of drought stress responses in large-and small-rooted rice lines: physiological, anatomical, and hormonal changes. Journal of Plant Growth Regulation, 43: 2922–2936.

Hou D., Liu K., Liu S., Li J., Tan J., Bi Q., Zhang A., Yu X., Bi J., Luo L. (2024): Enhancing root physiology for increased yield in water-saving and drought-resistance rice with optimal irrigation and nitrogen. Frontiers in Plant Science, 15: 1370297.

Huang S., Zhen H., Zheng Q. (2020): Characterization of eating quality and starch properties of two *Wx* alleles japonica rice cultivars under different nitrogen treatments. Journal of Integrative Agriculture, 19: 988–998.

Khan M., Al Azzawi T.N.I., Imran M., Hussain A., Mun B.G., Pande A., Yun B.W. (2021): Effects of lead (Pb)-induced oxidative stress on morphological and physio-biochemical properties of rice. Biocell, 45: 1413.

Koper K., de Oliveira M.V., Huß S., Hataya S., Soleymani F., Hawkins C., Rhee S.Y., Takasuka T.E., Nikoloski Z., Maeda H.A. (2025): Mapping multi-substrate specificity of Arabidopsis aminotransferases. Nature Plants, 11: 1863–1876.

Kusano M., Fukushima A., Redestig H., Saito K. (2011): Metabolomic approaches toward understanding nitrogen metabolism in plants. Journal of Experimental Botany, 62: 1439–1453.

Lee S., Masclaux-Daubresse C. (2021): Current understanding of leaf senescence in rice. International Journal of Molecular Sciences, 22: 4515.

Li X., Wang R., Zhou B., Wang X., Wang J., Zhao M., Li C. (2022): Characterization of root morphology and anatomical structure of spring maize under varying N application rates and their effects on yield. Agronomy, 12: 2671.

Li H.J., Li H.R., Zhang D.K., Jiang M.M., Cao J., Xu G.W. (2025): Irrigation methods and nitrogen-form interactions regulate starch-metabolising enzyme activity to improve rice yield and quality. Plant, Soil and Environment, 71: 185–201.

Li J., Yang S., Zhong Z., Xia T., Zhou W., Tu Z.,Chen Z.,Wang H., Dai Z., Jin G., Du Y. (2025): Effects of degree of milling on bran layer structure, physicochemical properties and cooking quality of brown rice. Food Chemistry, 462: 140847.

Liang H., Gu B., Wang T., Rong L., Sun W., Wu Z. (2022): Relationship between protein structure and eating quality of rice under different nitrogen application rate. Cereal Chemistry, 99: 692–703.

Liu H., Wang W., He A., Nie L. (2018): Correlation of leaf and root senescence during ripening in dry seeded and transplanted rice. Rice Science, 25: 279–285.

Liu Q., Chen S., Zhou L., Tao Y., Tian J., Xing Z., Wei H., Zhang H. (2022): Characteristics of population quality and rice quality of semi-waxy japonica rice varieties with different grain yields. Agriculture, 12: 241.

Liu A., Li Y., Yang L., Zhang Y., Liao S., Li X. (2024): Applying nitrogen fertilizer improves the indica rice (*Oryza sativa* L.) quality by coordinating enzyme activity and grain-filling rate. Cereal Chemistry, 101: 1043–1054.

Liu K., Chen Y., Li S., Wang W., Zhang W., Zhang H., Gu J., Yang J., Liu L. (2023): Differing responses of root morphology and physiology to nitrogen application rates and their relationships with grain yield in rice. The Crop Journal, 11: 618–627.

Liu J., Yang T., Zou J., Zou J., Wu L., Bao X., Zhang B. (2025): Effects of reduced nitrogen fertilizer application rates on grain yield and rice quality of early-and late-season dual-use rice in South China. The Journal of Agricultural Science, 163: 99–109.

Lopez-Valdivia I., Yang X., Lynch J.P. (2023): Large root cortical cells and reduced cortical cell files improve growth under suboptimal nitrogen in silico. Plant Physiology, 192: 2261–2275.

Lv R., Zhang W., Xie X., Wang Q., Gao K., Zeng Y., Pan X., Shang Q. (2022): Foliar application uniconazole enhanced lodging resistance of high-quality indica rice (*Oryza sativa* L.) by altering anatomical traits, cell structure and endogenous hormones. Field Crops Research, 277: 108425.

Lynch J.P., Galindo-Castañeda T., Schneider H.M., Sidhu J.S., Rangarajan H., York L.M. (2023): Root phenotypes for improved nitrogen capture. Plant and Soil, 10: 06301.

Ma Z., Chen X., Cao J., Yu J., Zhu Y., Li G., Xu F., Zhang H., Liu G., Wei H. (2025): Analysis of the effects of light and panicle fertilizer on rice eating quality based on morphological structural changes in starch and protein during cooking. International Journal of Biological Macromolecules, 305: 141121.

Meng F., Guo J., Feng N., Zheng D., Chen X., Chen Z., Jiang H., Jiang X. (2024): Beneficial effects of hemin on antioxidative capacity and anatomical characters of NaCl-stressed rice plants. Journal of Plant Growth Regulation, 43: 3743–3760.

Owusu E.A., Luthra K., Regonda B., Atungulu G. (2025): Effects of nitrogen application rates on the physicochemical properties of modern rice cultivars: a comprehensive study. Cereal Chemistry, 102: 999–1012.

Qi D., Chen S., Yue W., Duan Y. (2024): Leaf senescence characteristics and economic benefits of rice under alternate wetting and drying irrigation and blended use of polymer-coated and common urea. Frontiers in Plant Science, 15: 1444819.

Sachadyn-Król M., Materska M., Chilczuk B., Karaś M., Jakubczyk A., Perucka I., Jackowska I. (2016): Ozone-induced changes in the content of bioactive compounds and enzyme activity during storage of pepper fruits. Food Chemistry, 211: 59–67.

Salah A., Nwafor C.C., Han Y., Liu L., Rashid M., Batool M., El-Badri A.M., Cao C., Zhan M. (2022): Spermidine and brassinosteroid regulate root anatomical structure, photosynthetic traits and antioxidant defense systems to alleviate waterlogging stress in maize seedlings. South African Journal of Botany, 144: 389–402.

Salsinha Y.C.F., Rini D.S., Indradewa D., Purwestri Y.A., Fatikhasari Z., Lailaty I.Q., Wutsqa Y.U., Harijayanti D., Rachmawati D. (2023): Anatomical characteristics of the upland local Indonesian rice cultivars as structural protection against drought. Brazilian Journal of Botany, 46: 645–659.

Schneider H.M., Postma J.A., Wojciechowski T., Kuppe C., Lynch J.P. (2017): Root cortical senescence improves growth under suboptimal availability of N, P, and K. Plant Physiology, 174: 2333–2347.

Shi S., Ma Y., Zhao D., Li L., Cao C., Jiang Y. (2023): The differences in metabolites, starch structure, and physicochemical properties of rice were related to the decrease in taste quality under high nitrogen fertilizer application. International Journal of Biological Macromolecules, 253: 126546.

Shiono K., Ejiri M., Sawazaki Y., Egishi Y., Tsunoda T. (2024): Low nitrate under waterlogging triggers exodermal suberization to form a barrier to radial oxygen loss in rice roots. Plant Physiology, 196: 551–563.

Singh N., Pal N., Mahajan G., Singh S., Shevkani K. (2011): Rice grain and starch properties: effects of nitrogen fertilizer application. Carbohydrate Polymers, 86: 219–225.

Song Y., Dong M., Chen F., Hu Y., Zhu Y., Gu J., Chen P., Xie Y., Yuan C., Qiao Z., Yu Y., Cao P., Shi L., Wang Y., Zhang M. (2024): Effects of nitrogen fertilizer reduction combined with foliar fertilizer application on the physiological characteristics and yield of high-quality japonica rice. International Journal of Plant Production, 18: 239–254.

Srivastava A., Gupta A., Bishi S.K., Akhila P., Latha P.C., Subrahmanyam D., Brajenndra P., Anantha M.S., Ch S.R., Sakhare A.S., Bhadana V.P., Giri J., Nddraja C.N., Sundaram R.M., Mangrauthia S.K. (2025): Tolerance of *Oryza sativa* to low phosphate is associated with adaptive changes in root architecture and metabolic exudates. Plant Science, 353: 112415.

Subudhi P.K., Garcia R.S., Coronejo S., Tapia R. (2020): Comparative transcriptomic of rice genotypes with contrasting responses to nitrogen stress reveals genes influencing nitrogen uptake through the regulation of root architecture. International Journal of Molecular Sciences, 21: 5759.

Tavu L.E.J., Redillas M.C.F.R. (2025): Oxidative stress in rice (*Oryza sativa*): mechanisms, impact, and adaptive strategies. Plants, 14: 1463.

Turk H., Erdal S., Genisel M., Atici O., Demir Y., Yanmis D. (2014): The regulatory effect of melatonin on physiological, biochemical and molecular parameters in cold-stressed wheat seedlings. Plant Growth Regulation, 74: 139–152.

Uga Y., Ebana K., Abe J., Morita S., Okuno K., Yano M. (2009): Variation in root morphology and anatomy among accessions of cultivated rice (*Oryza sativa* L.) with different genetic backgrounds. Breeding Science, 59: 87–93.

Velikova V., Yordanov I., Edreva A.J.P.S. (2000): Oxidative stress and some antioxidant systems in acid rain-treated bean plants: protective role of exogenous polyamines. Plant Science, 151: 59–66.

Wang R., Sun C., Cai S., Liu F., Xie H., Xiong Q. (2023): Research progress in crop root biology and nitrogen uptake and use, with emphasis on cereal crops. Agronomy, 13: 1678.

Wang C., Jing W., Fa X., Gu J., Wang W., Zhu K., Zhang W., Gu J., Wang Z., Zhang J., Zhang H. (2025): Effect of nitrogen levels on grain yield and quality in improving mid-season japonica rice varieties. Journal of the Science of Food and Agriculture, 105: 3010–3023.

Wei G., Wang X., Wu Y., Liu F., Lan T., Liu Q., Lyu C., Kong F., Yuan J. (2025): Post-silking leaf senescence is delayed in low-N-tolerant maize cultivars under low N fertilization. The Crop Journal, 13: 246–256.

Xin W., Liu H., Zhao H., Wang J., Zheng H., Jia Y., Yang L., Wang X., Li J., Li X., Lei L., Zou D. (2021): The response of grain yield and root morphological and physiological traits to nitrogen levels in paddy rice. Frontiers in Plant Science, 12: 713814.

Xu C., Chen L., Chen S., Chu G., Wang D., Zhang X. (2020): Effects of rhizosphere oxygen concentration on root physiological characteristics and anatomical structure at the tillering stage of rice. Annals of Applied Biology, 177: 61–73.

Xu Y., Li K., Zhu K., Tian Y., Yu Q., Zhang W., Wang Z. (2021): Effect of nitrogen rates on the growth and grain yield of a leaf early-senescent rice mutant. Agronomy Journal, 113: 1503–1522.

Xu Y., Huang Y., Weng X., Traye I., Tang S., Jiang X., Zhu K., Zhang W., Zhang H., Wang Z., Yang J. (2025): Cooking and eating quality of rice as affected by nitrogen fertilizers and alternate wetting and moderate drying irrigation at panicle stage. Agricultural Water Management, 318: 109715.

Yang X., Li Y., Ren B., Ding L., Gao C., Shen Q., Guo S. (2012): Drought-induced root aerenchyma formation restricts water uptake in rice seedings supplied with nitrate. Plant Cell Physiology, 53: 495–504.

Ye M., Wang Z., Wu M., Li H., Gu J., Yang J., Zhang H., Zhang Z. (2024): Optimized leaf anatomy improves photosynthetic producing capacity of mid-season indica rice in the Yangtze River Basin during the genetic improvement. European Journal of Agronomy, 158: 127196.

York L.M., Galindo-Castañeda T., Schussler J.R., Lynch J.P. (2015): Evolution of US maize (*Zea mays* L.) root architectural and anatomical phenes over the past 100 years corresponds to increased tolerance of nitrogen stress. Journal of Experimental Botany, 66: 2347–2358.

Zhang D.K., Li Y.Y., Li H.R., Li H.J., Zhao X.H., Cao J., Xu G.W. (2025): Phosphorus application rates affect the grain yields of different phosphorus-tolerant rice cultivars by regulating grain filling and leaf senescence characteristics. Plant, Soil and Environment, 71: 363–380.

Zhang X., Xing Y., Wang Q., Yan G., Wang M., Liu G., Wang H., Huang B., Zhang J. (2020): Effects of long-term nitrogen addition and decreased precipitation on the fine root morphology and anatomy of the main tree species in a temperate forest. Forest Ecology and Management, 455: 117664.

Zhang J., Zhang Y.Y., Song N.Y., Chen Q.L., Sun H.Z., Peng T., Huang S., Zhao Q.Z. (2021): Response of grain-filling rate and grain quality of mid-season indica rice to nitrogen application. Journal of Integrative Agriculture, 20: 1465–1473.

Zhao T., Wang J., Li R., Zhang P., Guo X., Qi Y., Li Y., Cheng S., Ji J., He A., Ai Z. (2025): Effects of nitrogen fertilizer types and planting density on the yield and nitrogen use efficiency of salt-tolerant rice under salt stress conditions. Plants, 14: 501.

Zhen B., Li H., Niu Q., Qiu H., Tian G., Lu H., Zhou X. (2020): Effects of combined high temperature and waterlogging stress at booting stage on root anatomy of rice (*Oryza sativa* L.). Water, 12: 2524.

Zhou M., Yang J. (2023): Delaying or promoting? Manipulation of leaf senescence to improve crop yield and quality. Planta, 258: 48.

Zhu D.W., Zhang H.C., Guo B.W., Xu K., Dai Q.G., Wei H.Y., Gao H., Hu Y.J., Cui P.Y., Huo Z.Y. (2016): Effects of nitrogen level on yield and quality of japonica soft super rice. Journal of Integrative Agriculture, 16: 1018–1027.

Zhu S., Sun S., Zhao W., Yang X., Chen Z., Mao H., Sheng L. (2024): Comprehensive physiology and proteomics analysis revealed the resistance mechanism of rice (*Oryza sativa* L.) to cadmium stress. Ecotoxicology and Environmental Safety, 278: 116413.

Received: January 15, 2026
Accepted: March 12, 2026